Polycyclic Aromatic Hydrocarbon-induced Pulmonary Carcinogenesis in Cytochrome P450 (CYP)1A1- and 1A2-Null Mice: Roles of CYP1A1 and CYP1A2

Grady Gastelum [*,†] Weiwu Jiang,[†] Lihua Wang,[†] Guodong Zhou,[‡] Roshan Borkar,[§] Nagireddy Putluri,[§] and Bhagavatula Moorthy[*,†,1]

[*]Interdepartmental Program in Translational Biology and Molecular Medicine, Baylor College of Medicine, Houston, Texas 77030; and [†]Section of Neonatology, Department of Pediatrics, Baylor College of Medicine, Houston, Texas 77030; [‡]Institute of Biosciences and Technology, Texas A&M University, Houston, Texas 77030; and [§]Dan L. Duncan Cancer Center, Advanced Technology Core, Alkek Center for Molecular Discovery, Baylor College of Medicine, Houston, Texas 77030

Grady Gastelum and Weiwu Jiang contributed equally to this study.

[1]To whom correspondence should be addressed at Section of Neonatology, Department of Pediatrics, Baylor College of Medicine, 1102 Bates Ave, FC 530.04, Houston, TX 77030. Fax: (832) 825-3204. E-mail: bmoorthy@bcm.edu.

ABSTRACT

In 2019, lung cancer was estimated to be the leading cause of cancer deaths in humans. Polycyclic aromatic hydrocarbons (PAHs) are known to increase the risk of lung cancer. PAHs are metabolized by the cytochrome P450 (CYP)1A subfamily, comprised of the CYP1A1 and 1A2 monooxygenases. These enzymes bioactivate PAHs into reactive metabolites that induce mutagenic DNA adducts, which can lead to cancer. Past studies have investigated the role of CYP1A1 in PAH bioactivation; however, the individual roles of each CYP1A enzyme are still unknown. In this investigation, we tested the hypothesis that mice lacking the genes for *Cyp1a1* or *Cyp1a2* will display altered susceptibilities to PAH-induced pulmonary carcinogenesis. Wild-type, *Cyp1a1*-null (*Cyp1a1*$^{-/-}$), and *Cyp1a2*-null (*Cyp1a2*$^{-/-}$) male and female mice were treated with 3-methylcholanthrene for cancer initiation and tumor formation studies. In wild-type mice, CYP1A1 and 1A2 expression was induced by 3-methylcholanthrene. *Cyp1a1*$^{-/-}$ and *Cyp1a2*$^{-/-}$ mice treated with PAHs displayed a compensatory pattern, where knocking out 1 *Cyp1a* gene led to increased expression of the other. *Cyp1a1*$^{-/-}$ mice were resistant to DNA adduct and tumor formation, whereas *Cyp1a2*$^{-/-}$ mice displayed increased levels of both. UALCAN analysis revealed that lung adenocarcinoma patients with high levels of CYP1A2 expression survive significantly better than patients with low/medium expression. In conclusion, *Cyp1a1*$^{-/-}$ mice were less susceptible to PAH-induced pulmonary carcinogenesis, whereas *Cyp1a2*$^{-/-}$ mice were more susceptible. In addition, high CYP1A2 expression was found to be protective for lung adenocarcinoma patients. These results support the need to develop novel CYP1A1 inhibitors to mitigate human lung cancer.

Key words: chemical carcinogenesis; lung cancer; polycyclic aromatic hydrocarbons; 3-methylcholanthrene.

In 2019, for both men and women, lung cancer was estimated to be the leading cause of cancer-related deaths (American Cancer Society, 2019). Up to 90% of lung cancer cases are caused by the inhalation of tobacco smoke (World Health Organization (WHO) International Agency for Research on Cancer, 2004), which is known to contain significant levels of polycyclic aromatic

hydrocarbons (PAHs) (Grimmer et al., 1988). Additional sources of PAHs include outdoor air pollution from coal combustion and vehicle (VEH) emissions as well as the consumption of smoked meats and fish from polluted water sources (National Research Council, 1983; Pokhrel et al., 2018; Shi et al., 2016; Simko, 2002). Interestingly, when PAHs enter the body, they are initially termed procarcinogens because they require metabolic activation to become carcinogenic.

One of the most potent carcinogenic PAHs is 3-methylcholanthrene (MC) (Harvey, 1982). Upon entry into the cell, MC induces phase I (CYP1A1 and 1A2) and phase II enzymes by activating the Ah receptor (Moorthy et al., 2015). Cyp1a1 and Cyp1a2 are controlled by a bidirectional promoter, which results in the widespread expression of CYP1A1 and liver-specific expression of CYP1A2 (Jorge-Nebert et al., 2010). CYP1A-mediated metabolism is known to result in the bioactivation of PAHs, such as benzo(a)pyrene (BP) (Moorthy et al., 2015) and MC (Kondraganti et al., 2003; Lu et al., 1990; Wood et al., 1978), which in turn results in the formation of metabolic intermediates that can bind to DNA to form mutagenic DNA adducts (Kondraganti et al., 2003; Lu et al., 1990).

If not repaired, these DNA adducts can lead to mutations that alter tumor suppressor and/or oncogene expression (Hecht, 2003, 2012; Vaz et al., 2017). Previous studies have strongly correlated the presence of DNA adducts in human white blood (Tang et al., 2001) and bronchial cells (Ceppi et al., 2017) with a significantly increased risk of developing lung cancer. In addition, mouse studies have shown positive correlations between PAH-DNA adducts and pulmonary tumor formation (Phillips et al., 2015; Poirier and Beland, 1992). CYP1A enzymes are also known to play a key role in the detoxification of PAHs into nontoxic metabolites (Nebert et al., 2013; Uno et al., 2006). The metabolites are further metabolized by phase II enzymes such as epoxide hydrolase (Stiborová et al., 2014), NAD(P)H quinone oxidoreductase 1 (NQO1), UDP glucuronyl transferase, and glutathione S-transferases (Yeager et al., 2009).

Earlier, we reported that MC-treated rats showed persistent expression of CYP1A1 in both liver and extrahepatic tissues, such as lung and breast tissue, for up to 45 days after MC withdrawal (Moorthy, 2000). We also showed that the sustained induction of CYP1A1 is independent of the persistence of the parent compound (Moorthy, 2000). The long-term expression of CYP1A1 was found to occur in target organs of PAH-mediated carcinogenesis, such as the lung (O'Donnell et al., 2006), suggesting that persistent CYP1A1 expression might play a role in carcinogenesis. In subsequent mouse studies, we reported that MC elicits sustained upregulation of CYP1A1 and 1A2 in the liver and CYP1A1 in the lung. In addition, mice lacking the Cyp1a2 gene showed persistent expression of CYP1A1 in the lung, but to a much lesser extent in liver (Kondraganti et al., 2002), suggesting that CYP1A2 plays a role in the regulation of CYP1A1 expression by MC (Jiang et al., 2010). MC also caused the sustained expression of CYP1A1 in human hepatoma cells (Fazili et al., 2010).

The CYP1A enzymes, which share 80% sequence homology (Juvonen et al., 2020; Nukaya and Bradfield, 2009), may have resulted from a gene duplication event (Goldstone and Stegeman, 2006). However, little is known regarding the individual roles of CYP1A1 and 1A2 in PAH carcinogenesis. Furthermore, there are few studies regarding the existence of sex differences in PAH-mediated lung carcinogenesis (Ben-Zaken Cohen et al., 2007; Lingappan et al., 2013; Singh et al., 1998).

To this end, we tested the hypothesis that CYP1A1 and 1A2 play unique functional roles in DNA adduct formation and lung carcinogenesis mediated by PAHs. Specifically, we hypothesized that mice lacking the genes for Cyp1a1 or Cyp1a2 will display altered susceptibilities to PAH-induced pulmonary carcinogenesis and tumorigenesis. Because gender differences are known to exist in humans with regard to cancer susceptibility (Uppstad et al., 2011), we also tested the hypothesis that male and female mice will show differences in their susceptibility to MC-mediated lung carcinogenesis. This study will help inform future studies examining potential prophylactic therapies (Horley et al., 2017; Zhou et al., 2011) for PAH-induced lung cancer.

MATERIALS AND METHODS

Chemicals. MC was obtained from Toronto Research Chemicals (Cat No. M294460; Lot No. 4-DPP-71-3). MC was prepared using corn oil (CO) (Sigma; Cat No. C8267-500ml; Lot No.MKCF8882) as a vehicle. Methoxyresorufin (Cat No. 85707; Lot No. 64772) and ethoxyresorufin (Cat No. 85715; Lot No. CM8-115) were purchased from Molecular Probes (Freemont, California). Ethoxyresorufin, polyvinylidene difluoride (PVDF) membranes (Cat No. IPVH00010; Lot No. R6NA3434B), as well as the buffer components for electrophoresis and Western blotting were obtained from Bio-Rad Laboratories (Hercules, California). The primary monoclonal antibody against CYP1A1/1A2 was a gift from Dr P. E. Thomas (Rutgers University, New Brunswick, New Jersey). The NQO1 antibody was purchased from Santa Cruz (Cat No. sc-16464; Lot No. H0713). β-Actin (horseradish peroxidase, HRP) primary antibody was purchased from Santa Cruz (Cat No. sc-47778HRP; Lot No. J1916). The GRP78 primary antibody was purchased from Abcam (Cat No. ab21685). Goat anti-mouse IgG (Cat No. 170-6516) conjugated with HRP was purchased from Bio-Rad Laboratories. Donkey anti-goat IgG (Cat No. sc-2020; Lot No. H2113) conjugated with HRP was purchased from Santa Cruz Biotechnology. Blotting grade blocker (milk) was purchased from BIO RAD (Cat No. 170-6404). Bovine serum albumin (BSA) was purchased from VWR (Cat No. 0332-100G; Lot No. 18J2556269). [γ-^{32}P] ATP was purchased from PerkinElmer Life and Analytical Sciences (Waltham, Massachusetts). The MC metabolite standards 1-hydroxy-3-MC (1-OH-MC), 2-hydroxy-3-MC (2-OH-MC), 11-hydroxy-3-MC (11-OH-MC), 11,12-dihydro-11,12-dihydroxy-3-MC (MC-11.12-diol), 1-one-3-MC (MC-1-one), 11,12-epoxy-11,12-dihydro-3-MC (MC-11,12-didydroepoxide), 11,12-dione-3-MC (MC-11,12-dione), and 11,12-dialdehyde-3-MC (MC-11,12-dialdehyde) were purchased from Chemsyn (Lawrence, Kansas).

Animals. Our animal protocol (AN-907) was approved by the Institutional Animal Care and Use Committee of Baylor College of Medicine, and the animal experiments were conducted in strict accordance with federal guidelines for the humane care and use of laboratory animals. A/J wild-type (WT) mice (RRID: IMSR_ARC: A/J) were obtained from Jackson Laboratories and Cyp1a1- and Cyp1a2-null mice (A/J) were generated by backcrossing C57BL/6J/Sv129 Cyp1a1- and Cyp1a2-null mice with WT A/J mice for 10 generations. The Cyp1a1-null ($Cyp1a1^{-/-}$) mouse breeding pairs were generously donated by Dr Daniel Nebert. The Cyp1a2-null ($Cyp1a2^{-/-}$) mouse breeding pairs were obtained from Dr Frank J. Gonzalez (National Cancer Institute, Bethesda, Maryland). The animals were housed at the Feigin Center animal facility at Baylor College of Medicine. Animals were maintained in a facility with a 12-h day/night cycle in temperature and humidity-controlled rooms. Purified tap water and

rodent chow (Purina Rodent Lab Chow No. 5001 from Purina Mills, Richmond, Indiana) were available to mice *ad libitum*. Mice used in the long-term tumorigenesis study were switched to AIN-76 semipurified pelleted diet after treatment and for the remainder of the study (MP Biomedicals; Cat No. 905453).

PAH exposure and tissue harvesting. MC is a prototypical PAH used to study mechanisms by which PAHs cause tumorigenesis in mice *in vivo*. The yearly amount of PAHs, such as BP, inhaled by smokers is 66.4 μg and can be increased through additional exposures such as outdoor air pollution and consumption of certain foods (eg, smoked meat) (Moorthy *et al.*, 2015). This extrapolates to an environmental dose of 230 ng/kg, and a total human exposure of 7 mg per year (Moorthy *et al.*, 2015). Therefore, we chose to treat our animals with a single dose of MC at 40 μmol/kg. This dose corresponds to roughly 268 μg/ mouse, which is much lower than the annual human consumption of PAHs (approximately 7 mg). This dose of MC (40 μmol/kg) was similar to those used by other investigators to induce lung tumors (Henry *et al.*, 1981). Based on these past studies, male and female mice, between the age of 8 and 10 weeks old, were randomized into 2 treatment groups that received either CO (vehicle) or MC (40 μmol/kg). At this dosage, mice were given a single intraperitoneal injection. For the DNA adduct study (Figure 3), the mice were treated with MC (100 μmol/kg) via 4 consecutive daily ip injections. For the cancer initiation study, MC-treated animals were sacrificed at 1-, 8-, and 15-days post-PAH exposure, whereas the CO-treated animals were sacrificed only at the 1-day post exposure timepoint. At each timepoint, the liver and lung tissues were snap-frozen in liquid nitrogen (−80°C) for later DNA, RNA, and protein isolation. Once processed, the samples were analyzed for protein expression (Western blotting), RNA expression real-time PCR (RT-PCR), DNA adduct formation (^{32}P-postlabeling), and enzyme activity (ethoxyresorufin O-deethylase, EROD/methoxyresorufin *O*-demethylase, MROD). For the tumorigenesis study, MC-treated animals were sacrificed 32-weeks post-MC or vehicle exposure. Liver samples were snap-frozen (−80°C) in liquid nitrogen for later analysis. Lungs were perfused with zinc formalin, fixed for 24 h, and then stored in 70% ethanol at 4°C. The pulmonary tumor counts were obtained for tumor multiplicity and incidence analysis.

DNA isolation and adduct detection. Genomic DNA was isolated from liver and lung tissues. The nuclease P1-enhanced bisphosphate version of the ^{32}P-postlabeling method was used for the detection of DNA adduct formation, with modification of the chromatographic conditions analysis, as described previously (Reddy and Randerath, 1986; Zhou *et al.*, 2011).

RNA isolation and RT-PCR. Frozen lung and liver tissue samples were used for RNA isolation, using the Direct-zol RNA MiniPrep kit (Zymo Research; Cat No. R2072). We utilized RT-PCR to analyze the hepatic and pulmonary mRNA expression levels. For RT-PCR experiments the TaqMan RNA-to-C_T 1-Step Kit (Cat No. 4392938) and TaqMan Gene Expression Assays (Ref No. 4331182) were used with the Applied Biosystems PRISM 7700 system. The delta-delta Ct method was used to calculate the target and reference (18S) gene expression. All RT-PCR values were normalized to those of vehicle-treated WT animals. The following TaqMan primers were used: Cyp1a1 (Hs00153120_m1 CYP1A1), Cyp1a2 (Hs00167927_m1 CYP1A2), Nqo1 (Hs00168547_m1 NQO1), and 18S (Hs99999901_s1 18S).

Protein isolation and Western blotting. Cytosolic and microsomal samples were isolated from lung and liver tissues to analyze NQO1 and CYP1A1/1A2, respectively. Calcium chloride precipitation was used to isolate liver microsomes (Cinti *et al.*, 1972; Moorthy, 2000; Moorthy *et al.*, 1993). Lung microsomes were isolated by differential centrifugation (Matsubara *et al.*, 1974). Western blotting analysis was used to determine the protein expression levels in lung and liver tissues. GRP78 was used as a loading control for microsomal samples (CYP1A1/1A2) and β-actin was used as a loading control for cytosolic targets (NQO1). Sodium dodecyl sulfate polyacrylamide gel electrophoresis was used to analyze the liver and lung protein samples. Proteins were transferred to PVDF membranes. The CYP1A1/1A2 membranes were blocked with 5% milk, whereas the NQO1 blots were blocked with 5% BSA. The membranes were then incubated with primary antibodies, HRP-tagged secondary antibodies and quantified using BioRad ChemiDoc Touch and Image Lab Software (BioRad, Cat No. 12003153). All representative Western blots (Figs. 1G, 1N, 2D, and 2H) were used for the protein analysis in their respective figures.

Enzyme assays. EROD activity was used as a marker of CYP1A1 activity, whereas MROD activity was used as a marker of CYP1A2 activity in liver and lung tissues, as described previously (Moorthy *et al.*, 1997).

Mass spectrometry. Liver and lung tissue samples were homogenized in phosphate-buffered saline at a final concentration of 100 mg/ml (wt/vol), and then 100 μl of homogenate was extracted twice using 2 ml of tertiary butyl ether. The extracts were combined and evaporated to dryness. The dried extracts were reconstituted with 100 μl of methanol and analyzed by LC-MS/MS. MC and its metabolites were detected in liver and lung tissues with a 6490 Triple Quadrupole LC-MS/MS (Agilent Technologies, Santa Clara, California) equipped with an Agilent HPLC system with a quaternary pump, a degasser, an autosampler and a column compartment. The data acquisition was performed with MassHunter software (Agilent Technologies). The compounds were detected via positive electrospray ionization in selected monitoring mode (SRM). MC and its metabolites were separated on a Luna C5, 5 μ 2 × 50 mm analytical column (Phenomenex, Torrance, California) at 50°C. The initial mobile phase consisted of 0.2% formic acid in water (A) and methanol (B) with gradient elution at a flow rate of 0.2 ml/min and the injection volume was 2 μl. The gradient program was as follows (min/%B): 0/70, 0.5/70, 3.5/98, 5.5/98, and 7.0/70. The specific SRM transitions were as follows: MC *m/z* 269.1 > 254, 1-hydroxy-3-methylcholanthrene *m/z* 266.8 > 252, 2-hydroxy-3-methylcholanthrene *m/z* 267.1 > 252, 11-hydroxy-3-methylcholanthrene *m/z* 285.2 > 255, 3-methylcholanthrene-1-one *m/z* 283.2 > 254.2, 11,12-epoxy-11, 12-dihydro-3-methylcholanthrene *m/z* 285.1 > 269.9, 11,12-dione-3-methylcholanthrene *m/z* 321 > 257, 3-methylcholanthrene-11,12-dihydrodiol *m/z* 285.3 > 269.9, and 3-methylcholanthrene-11,12-dialdehyde *m/z* 255 > 239.9.

UALCAN/TCGA analysis. UALCAN is an interactive web resource for analyzing cancer omics data from sources such as The Cancer Genome Atlas (TCGA). UALCAN was used to analyze CYP1A2 RNA expression in lung cancer patients. Specifically, we evaluated the effect of high CYP1A2 expression (upper quartile) versus medium/low CYP1A2 expression (lower 2 quartiles) on patient survival in lung adenocarcinoma (LUAD) cases. We also utilized UALCAN to generate the Kaplan-Meier graphs shown in Figure 3 (Chandrashekar *et al.*, 2017).
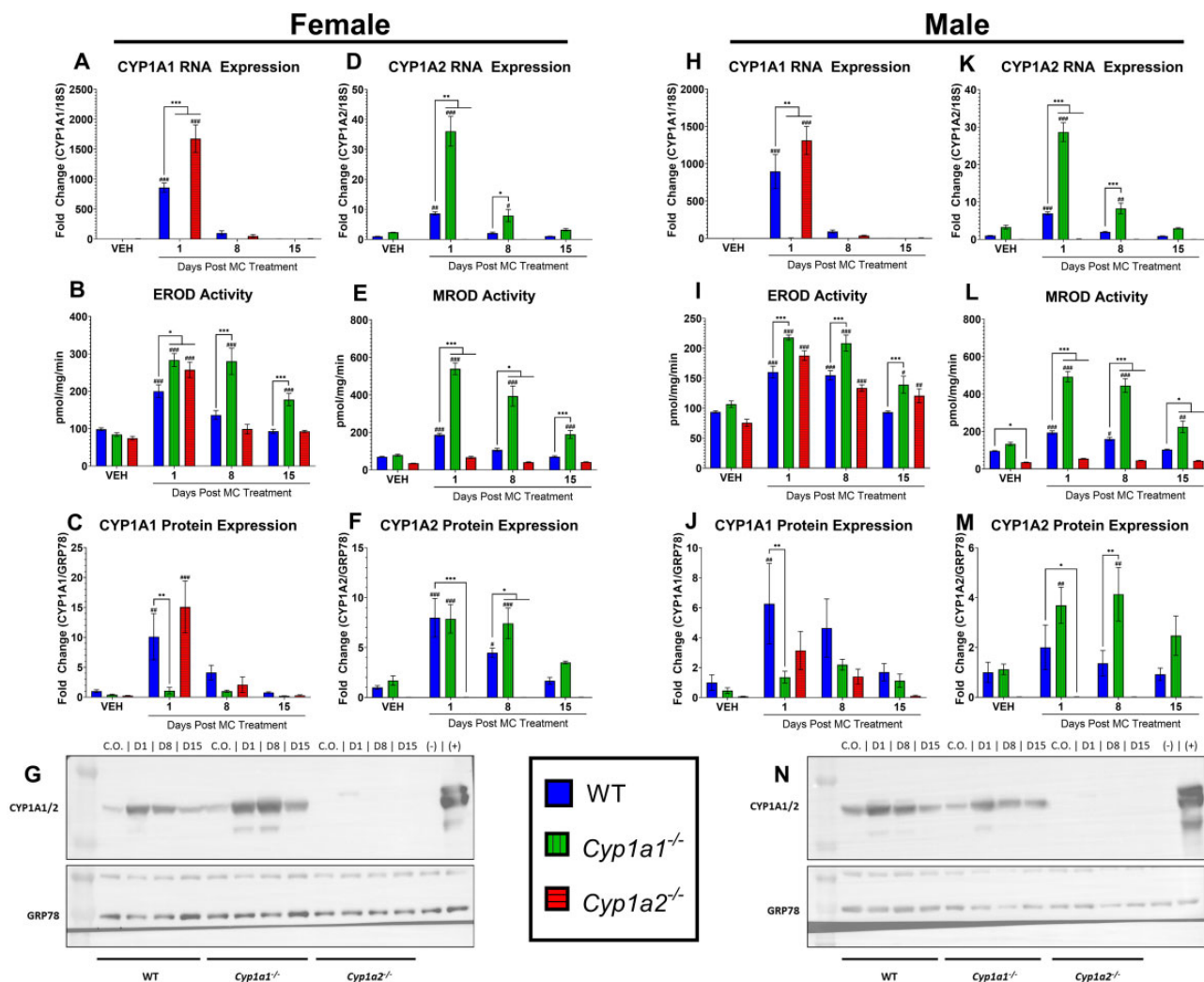
Figure 1. Effect of 3-methylcholanthrene (MC) on hepatic *CYP1A* gene expression, enzyme activities, and protein expression. Male and female wild-type (WT), $Cyp1a1^{-/-}$, and $Cyp1a2^{-/-}$ mice were administered the vehicle (VEH) corn oil (CO) or a single dose of MC (40 μmol/kg). Mice were sacrificed at 1, 8, and 15 days after CO or MC treatment. The following parameters were determined in liver tissue from at least 3 individual animals per treatment group, as described in the Materials and Methods section. Female CYP1A1 RNA expression (A), ethoxyresorufin O-deethylase (EROD) activity (B), and protein expression (C). Female CYP1A2 RNA expression (D), methoxyresorufin O-demethylase (MROD) activity (E), and protein expression (F). Representative female CYP1A1/1A2 Western blot (G). Male CYP1A1 RNA expression (H), EROD activity (I), and protein expression (J). Male CYP1A2 RNA expression (K), MROD activity (L), and protein expression (M). Representative male CYP1A1/1A2 Western blot (N). Significant differences between WT and knockout mice at each timepoint are indicated by $^*p < .05$, $^{**}p < .01$, and $^{***}p < .001$. Significant differences between vehicle and MC-treated mice at each timepoint are indicated by $\#p < .05$, $\#\#p < .01$, and $\#\#\#p < .001$.

Statistical analyses. Cancer initiation ($n = 3–4$) and tumorigenesis ($n = 8–14$) studies were analyzed with GraphPad Prism 8 via 2-way ANOVA (Dunnett's multiple comparison test). All graphs show the mean value ± SEM. For each genotype, we determined target gene (RNA, protein, enzyme activity) induction over the vehicle control by comparing the vehicle controls to the results obtained at the 1-, 8-, and 15-days post-MC timepoints. For each timepoint, $Cyp1a1^{-/-}$ and $Cyp1a2^{-/-}$ mice were compared with their WT controls.

RESULTS

Hepatic CYP1A1/1A2 RNA, Protein, and Enzyme Activity
For the cancer initiation study, we treated male and female mice of all 3 genotypes with a single dose of CO (vehicle) or MC and sacrificed the animals at 1-, 8-, and 15-days post-MC exposure. CYP1A1 and 1A2 RNA and protein were measured using RT-PCR and Western blotting, respectively. The EROD and MROD activities were used as markers of CYP1A1 and 1A2, respectively. At 1-day post exposure, female WT mice showed an 859.9-fold increase in CYP1A1 RNA expression ($p < .0001$), a 1.03-fold increase in enzyme activity ($p = .0002$), and a 9.1-fold increase in protein expression ($p = .0035$) compared with baseline levels (Figs. 1A–C). They also displayed a 7.7-fold increase in CYP1A2 RNA expression ($p = .0025$), a 1.7-fold increase in enzyme activity ($p = .004$), and a 6.99-fold increase in protein expression ($p < .0001$) compared with baseline levels (Figs. 1D–F; representative Western blot Figure 1G). At 1-day post exposure, male WT mice showed an 896.3-fold increase in CYP1A1 RNA expression ($p < .0001$), a 0.71-fold change in EROD activity ($p < .0001$), and a 5.3-fold increase in protein expression ($p = .0058$) compared with the baseline levels (Figs. 1H–J). Male WT mice also displayed a 5.96-fold increase in CYP1A2 RNA expression ($p = .0002$) and a 1.04-fold change in enzyme activity ($p = .0005$) compared with the baseline levels at 1-day post

exposure; however, there was no significant change in protein expression ($p = .44$) (Figs. 1K–M; representative Western blot, Figure 1N). These increases mostly declined by day 8 in both female and male WT mice.

We found that compared with WT mice, $Cyp1a1^{-/-}$ female mice displayed 316% ($p < .0001$) and 271% ($p = .001$) increases in the levels of hepatic CYP1A2 RNA at 1- and 8-days post-MC exposure, respectively (Figure 1D). $Cyp1a1^{-/-}$ female mice also showed a 167%–268% increase in MROD activity through day 15 ($p \leq .0002$) compared with WT mice (Figure 1E). This was accompanied by an increase in hepatic CYP1A2 protein expression above baseline levels on days 1 ($p < .0001$) and 8 ($p = .0002$) post exposure (Figure 1F; representative Western blot Figure 1G), with expression levels on day 8 being 66% higher than those of WT mice ($p = .041$). Compared with WT mice, $Cyp1a1^{-/-}$ male mice showed 312% and 310% increases in CYP1A2 RNA levels 1- and 8-days post exposure ($p < .0001$), respectively (Figure 1K). MROD activity was also found to be above the levels observed in WT mice, with male $Cyp1a1^{-/-}$ mice displaying 119%–178% higher activity ($p < .0001$) at 1-, 8-, and 15-days post exposure (Figure 1L). CYP1A2 protein levels were above the baseline at days 1 and 8 post exposure in $Cyp1a1^{-/-}$ mice, with the day 8 levels being 203.3-fold higher than those of WT mice (Figure 1M; representative Western blot, Figure 1N).

Female $Cyp1a2^{-/-}$ mice displayed a 95% increase in CYP1A1 RNA expression ($p < .0001$) and a 29% increase in EROD activity ($p = .025$) at 1-day post exposure compared with WT mice (Figs. 1A and 1B). Female $Cyp1a2^{-/-}$ mice failed to show an increase in CYP1A1 protein (Figs. 1C and 1G). Male $Cyp1a2^{-/-}$ mice showed a significant increase in 46% in CYP1A1 RNA expression ($p = .0039$) compared with WT mice at day 1 post-MC exposure (Figure 1H). The EROD activity in male $Cyp1a2^{-/-}$ mice was 59.9%–148.4% above baseline levels ($p = .0016$) for up to 15-days post exposure (Figure 1I). Male $Cyp1a2^{-/-}$ mice also failed to show an increase in CYP1A1 protein (Figs. 1J and 1N).

Pulmonary CYP1A1 RNA, Protein, and Enzyme Activity

In WT female mice, we observed a significant 280.4-fold ($p < .0001$) and 74.6-fold ($p < .0001$) increase in CYP1A1 RNA expression compared with baseline at 1- and 8-days post-MC exposure, respectively (Figure 2A). We also observed a 0.24-fold ($p = .0061$) and 0.82-fold ($p < .0001$) increase in EROD activity compared with baseline at 1- and 8-days post exposure, respectively (Figure 2B). WT female protein levels showed an 83.7-fold ($p < .0001$) increase above baseline levels at 8-days post exposure (Figure 2C; representative Western blot, Figure 2D). The WT male mice showed a 280.4-fold ($p < .0001$) and 74.6-fold ($p < .0001$) increase in CYP1A1 RNA expression at 1- and 8-days post-MC exposure (Figure 2E). The male mice also showed a 1.2-fold ($p = .0003$) increase in EROD activity compared with baseline 1-day post exposure (Figure 2F). This was accompanied by a 154.1-fold ($p = .037$) and 259-fold ($p = .0005$) increase in CYP1A1 protein compared with the baseline levels at 1- and 8-days post exposure (Figure 2G; representative Western blot, Figure 2H).

Male and female $Cyp1a1^{-/-}$ mice failed to induce expression of pulmonary CYP1A1 RNA, protein or enzyme activity when compared with vehicle-treated control mice, as expected (Figure 2). Female $Cyp1a2^{-/-}$ mice showed a 38.7-fold ($p < .0001$) and 6.2-fold ($p = .0047$) increase in CYP1A1 RNA over baseline levels at 1- and 8-days post exposure, respectively (Figure 2A). When compared with WT mice, the female $Cyp1a2^{-/-}$ mice displayed a 22% increase in RNA levels ($p < .0001$) at 1-day post-MC exposure (Figure 2A). EROD activity was increased over baseline levels by 0.42-fold ($p < .0001$) at 1-day post exposure and 0.66-

fold ($p < .0001$) at 8-days post exposure in female $Cyp1a2^{-/-}$ mice (Figure 2B). At 1-day post exposure, female $Cyp1a2^{-/-}$ mice displayed a 30% increase ($p < .0001$) in EROD activity compared with WT mice (Figure 2B).

MC treatment of female $Cyp1a2^{-/-}$ mice also led to an induction of CYP1A1 protein expression over baseline levels by 18.6-fold ($p = .0007$) and 29.8-fold ($p < .001$) at 1- and 8-days post exposure, respectively (Figure 2C).

Similar to their female counterparts, male $Cyp1a2^{-/-}$ mice showed a significant induction of CYP1A1 RNA over baseline levels by 47.5-fold ($p < .0001$) and 6.1-fold ($p = .0037$) at 1- and 8-days post exposure, respectively (Figure 2E). When compared with WT mice, $Cyp1a2^{-/-}$ mice had a 24% increase ($p < .0001$) in CYP1A1 RNA at 1-day post exposure (Figure 2E). Enzyme activity assays revealed that $Cyp1a2^{-/-}$ male mice-induced EROD activity above baseline activity by 0.79-fold ($p = .0008$) and 0.51-fold ($p = .036$) at 1- and 8-days post exposure, respectively (Figure 2F). The level of CYP1A1 protein in male $Cyp1a2^{-/-}$ mice was increased 41.5-fold ($p < .0001$) over baseline at 8-days post-MC exposure (Figure 2G). This expression of CYP1A1 in $Cyp1a2^{-/-}$ mice was 60% higher ($p = .023$) than that in WT male mice at day 8 (Figure 2G). Although sex-specific differences do exist, our data suggest that there is a compensatory CYP1A1/1A2 response to PAH exposure as seen in the liver. Overall, $Cyp1a2^{-/-}$ mice showed sustained expression of CYP1A1 RNA and protein, and increases in CYP1A1 activities for up to 24 h in females and up to 15 days in males (Figure 2).

PAH-induced DNA Adduct Formation

To investigate whether $Cyp1a1^{-/-}$ or $Cyp1a2^{-/-}$ mice were more susceptible to carcinogenesis, we treated mice with MC and used ^{32}P-postlabeling to determine DNA adduct formation in liver and lung tissues. MC treatment gave rise to 11 different adduct spots in both the liver and lung that were not found in vehicle-treated controls (Figure 3A). Male and female $Cyp1a1^{-/-}$ mice showed similar pulmonary DNA adduct levels at day 8 (Figs. 3B and 3C). At 15-days post exposure, female $Cyp1a1^{-/-}$ mice showed a 122.9% increase ($p = .0004$) in DNA adduct formation compared with WT mice (Figure 3B), whereas males showed a 61% decrease ($p = .022$) (Figure 3C). Hepatic samples revealed that female $Cyp1a2^{-/-}$ mice harbored 97%–136% more hepatic DNA adducts than their WT counterparts at 1- ($p = .044$), 8- ($p < .0001$), and 15-days ($p = .0009$) post-MC exposure (Figure 3D). Similarly, male $Cyp1a2^{-/-}$ mice harbored 62%–162% more hepatic DNA adducts ($p < .05$) than their WT counterparts at 1- ($p = .0006$), 8- ($p = .0002$), and 15-days ($p = .017$) post-MC exposure (Figure 3E). $Cyp1a1^{-/-}$ male and female mice had approximately the same level of hepatic DNA adducts as WT mice.

Among the adduct spots, spot 7 (Figure 3A) represented adducts derived from 7,8-epoxy-7,8,9,10-tetrahydro-(1 or 2), and 7,8-epoxy-7,8,9,10-tetrahydro-(1 or 2), 9,10-trihydroxy-3-hydroxy-MC, which are the ultimate carcinogenic metabolites, based on chromatographic mobility of the adduct spots (Lu et al., 1990). The adducts represented by spot 8 (Figure 3A), were probably derived from the diol-epoxide pathway, based on its close proximity to spot 7 (Figure 3A). Adduct spots 7 and 8, which represent the binding of the ultimate carcinogenic metabolite of MC (ie, diol-epoxides), were formed to a remarkable extent in WT mice at each timepoint. A reduction in these spots was found in both male and female $Cyp1a1^{-/-}$ mice and was enhanced in $Cyp1a2^{-/-}$ mice (Supplementary Figure 1).
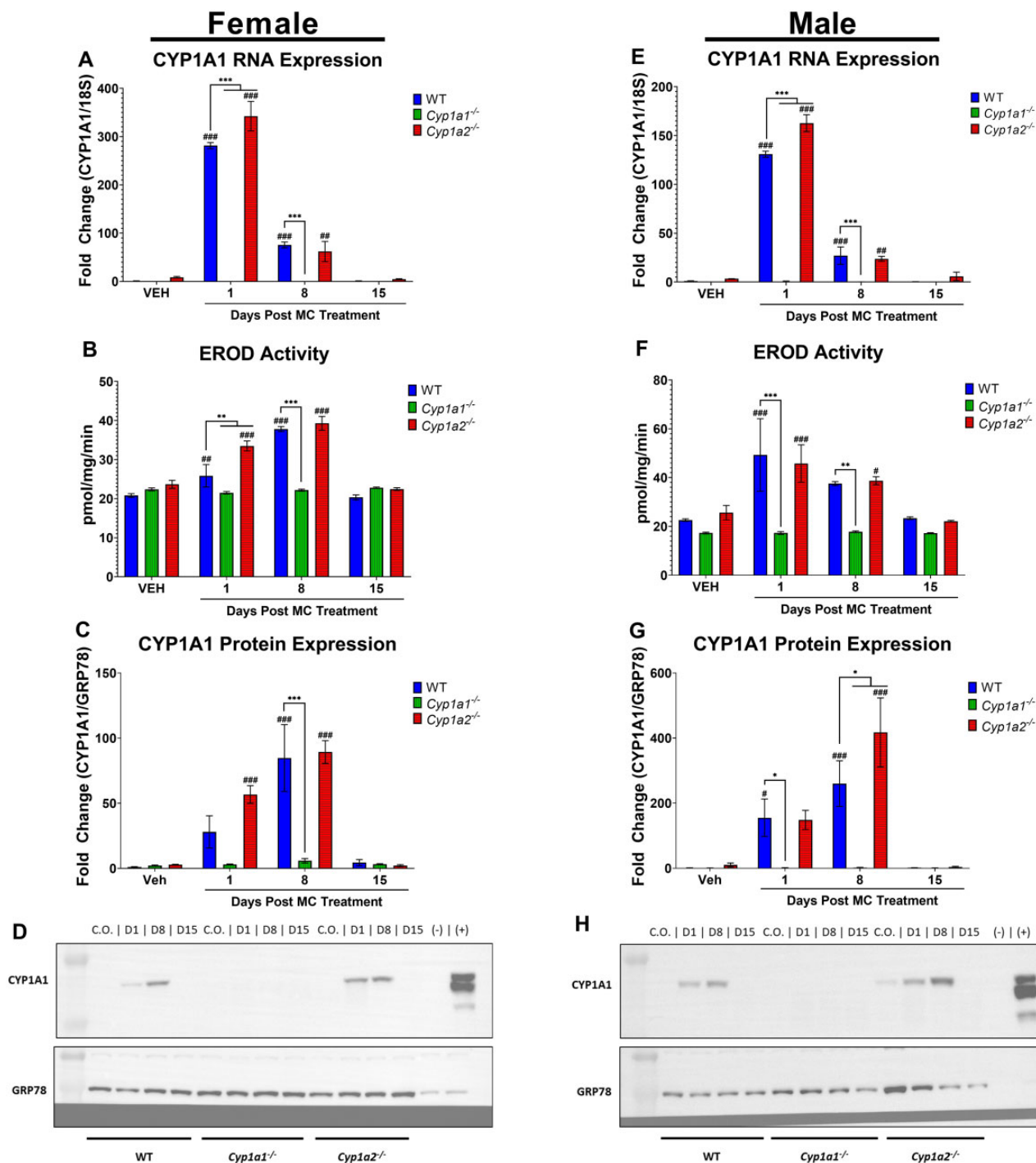
Figure 2. Effect of 3-methylcholanthrene (MC) on pulmonary CYP1A1 gene expression, ethoxyresorufin O-deethylase (EROD) activities, and protein expression. Mice were treated as previously described in Figure 1. Female CYP1A1 RNA expression (A), EROD activity (B), and protein expression (C). Representative blot of female CYP1A1 protein expression (D). Male CYP1A1 RNA expression (E), EROD activity (F), and protein expression (G). Representative blot of male CYP1A1 protein expression (H). Significant differences between wild-type (WT) and knockout mice at each timepoint are indicated by $*p < .05$, $**p < .01$, and $***p < .001$. Significant differences between vehicle (VEH)- and MC-treated mice at each timepoint are indicated by $\#p < .05$, $\#\#p < .01$, and $\#\#\#p < .001$.

Pulmonary NQO1 Expression

In the lung, NQO1 expression was mostly similar between CO- and MC-treated male and female WT mice (Figure 4), with the exception of NQO1 RNA in male WT mice at 1-day post exposure (Figure 4D; $p = .014$). Female $Cyp1a1^{-/-}$ mice showed a 1.9-fold ($p < .0001$) increase in NQO1 RNA levels compared with vehicle controls 1-day post exposure and a 0.49-fold increase 8-days ($p = .0085$) post exposure (Figure 4A). $Cyp1a2^{-/-}$ females showed only a 1.6-fold increase in the expression of NQO1 RNA compared with baseline levels at 1-day ($p < .0001$) post exposure (Figure 4A). Female $Cyp1a1^{-/-}$ mice displayed an increase in NQO1 protein above baseline levels (Figure 4B) at 8- ($p = .0002$) and 15-days ($p = .0015$) post exposure, with NQO1 protein levels being 77% higher in $Cyp1a1^{-/-}$ female mice than in WT animals
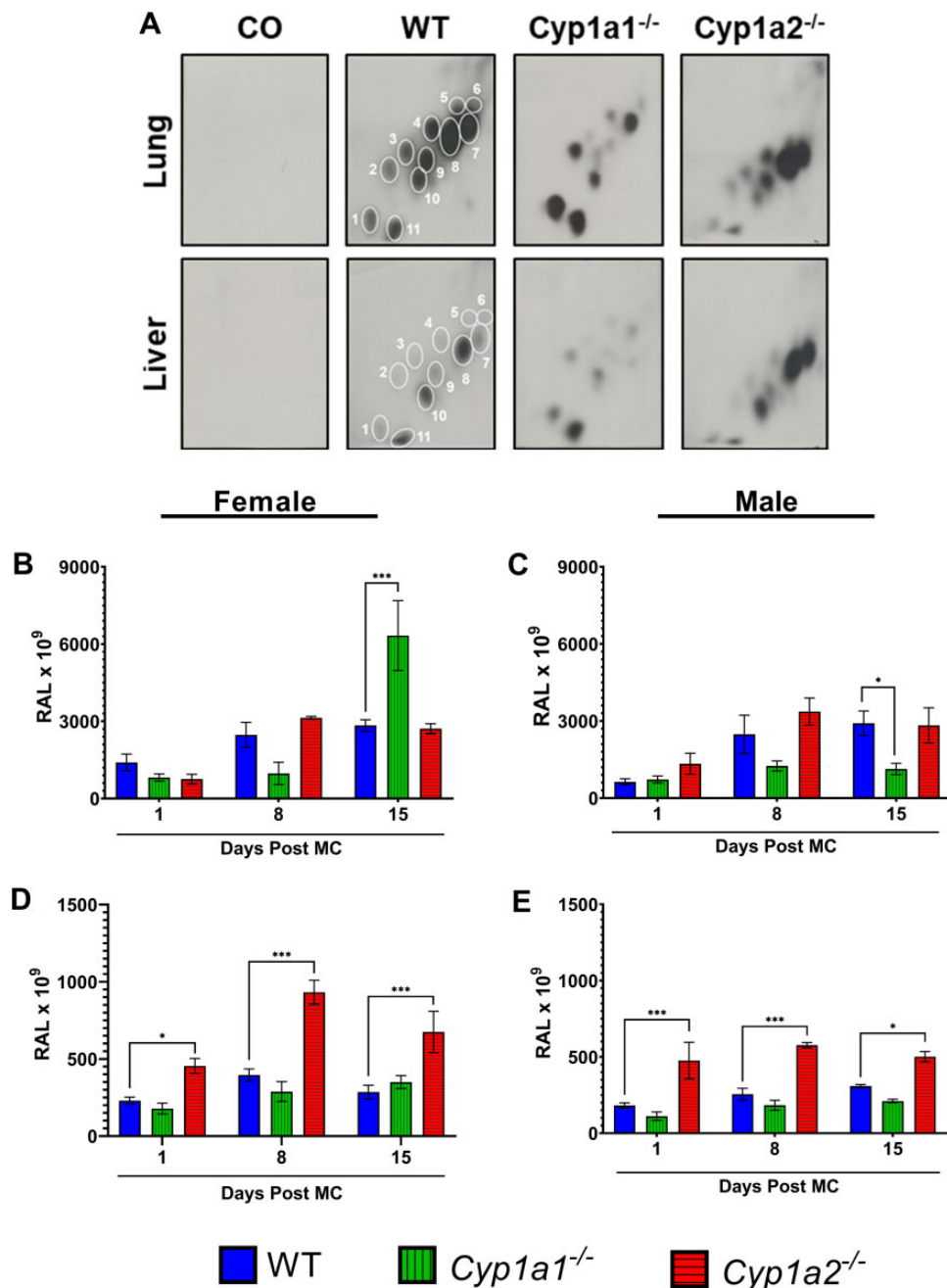
Figure 3. 3-Methylcholanthrene (MC)-induced hepatic and pulmonary DNA adduct formation. Male and female wild-type (WT), $Cyp1a1^{-/-}$, and $Cyp1a2^{-/-}$ mice were given daily ip injections of MC (100 μmol/kg) for 4 consecutive days and then sacrificed at 1-, 8-, and 15-days post-MC exposure. Representative pattern of MC-induced DNA adducts (A). Female (B) and male (C) pulmonary DNA adduct levels. Female (D) and male (E) hepatic DNA adduct levels. ^{32}P-postlabeling was used to detect DNA adducts in liver and lung tissues, as described in the Materials and Methods section. Values represent the mean Relative Adduct Levels (RALs) × 10^9 ± SEM ($n = 3$). Dunnett's multiple comparisons test was used to compare the knockout animals with their WT counterparts; significant differences are indicated by $^*p < .05$, $^{**}p < .01$, and $^{***}p < .001$.

at 15-days post exposure ($p = .023$). A representative Western blot image used in our analysis is provided (Figure 4C). The NQO1 RNA level (Figure 4D) was found to be higher than in vehicle controls 1-day post exposure in male $Cyp1a1^{-/-}$ mice (2.3-fold [$p < .0001$]) and $Cyp1a2^{-/-}$ mice (1.1-fold [$p = .028$]). $Cyp1a1^{-/-}$ male mice displayed a 1.46-fold ($p < .0001$) and 1.65-fold ($p = .0014$) increase in NQO1 RNA compared with their WT counterparts at 1- and 8-days post exposure, respectively (Figure 4D). Male $Cyp1a1^{-/-}$ mice showed an increase in NQO1 protein levels

(Figure 4E) of 2.0- and 1.7-fold compared with that in vehicle-treated mice at 8- ($p = .01$) and 15-days ($p = .028$) post exposure. A representative Western blot image that was used in our analysis is provided (Figure 4F).

Pulmonary and Hepatic Metabolomics

To investigate whether our knockout models had altered hepatic or pulmonary MC metabolite levels, we used LC-MS/MS to analyze the levels of MC and 8 known metabolites (Figs. 5 and
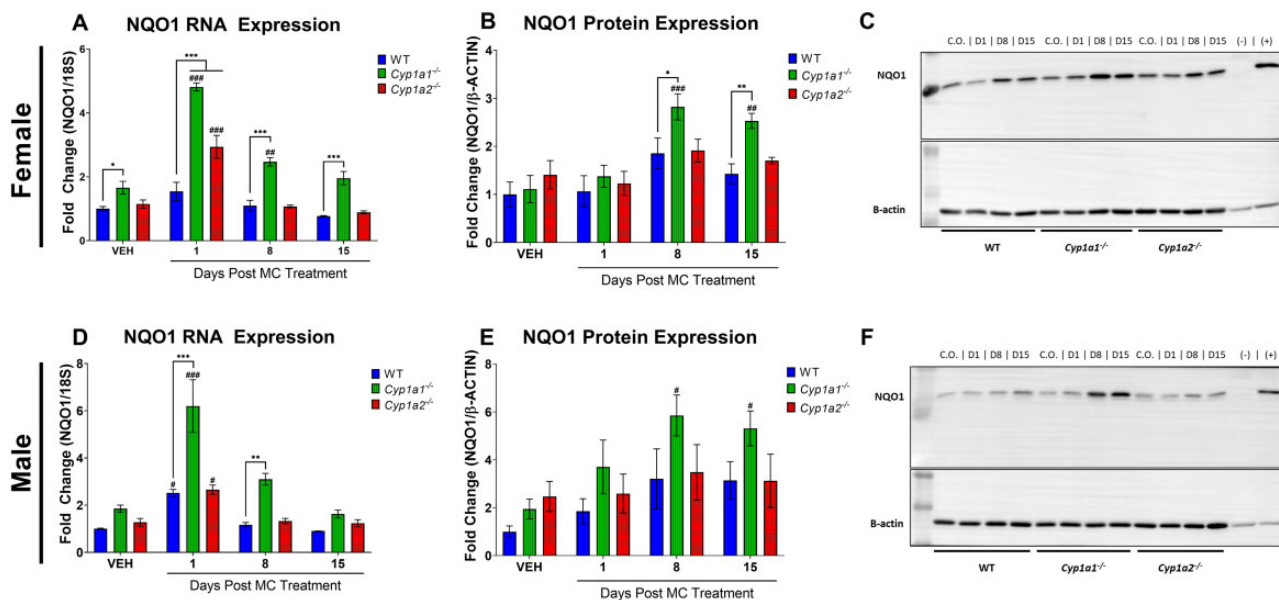
Figure 4. Effect of 3-methylcholanthrene (MC) on pulmonary NQO1 expression. Mice were treated as described in Figure 1. Female NQO1 RNA expression (A), protein expression (B), and representative blot of NQO1 protein expression (C). Male NQO1 RNA expression (D), protein expression (E), and representative blot of NQO1 protein expression (F). Significant differences between wild-type (WT) and knockout mice at each timepoint are indicated by $^*p < .05$, $^{**}p < .01$, and $^{***}p < .001$. Significant differences between vehicle (VEH) and MC-treated mice at each timepoint are indicated by $\#p < .05$, $\#\#p < .01$, and $\#\#\#p < .001$.
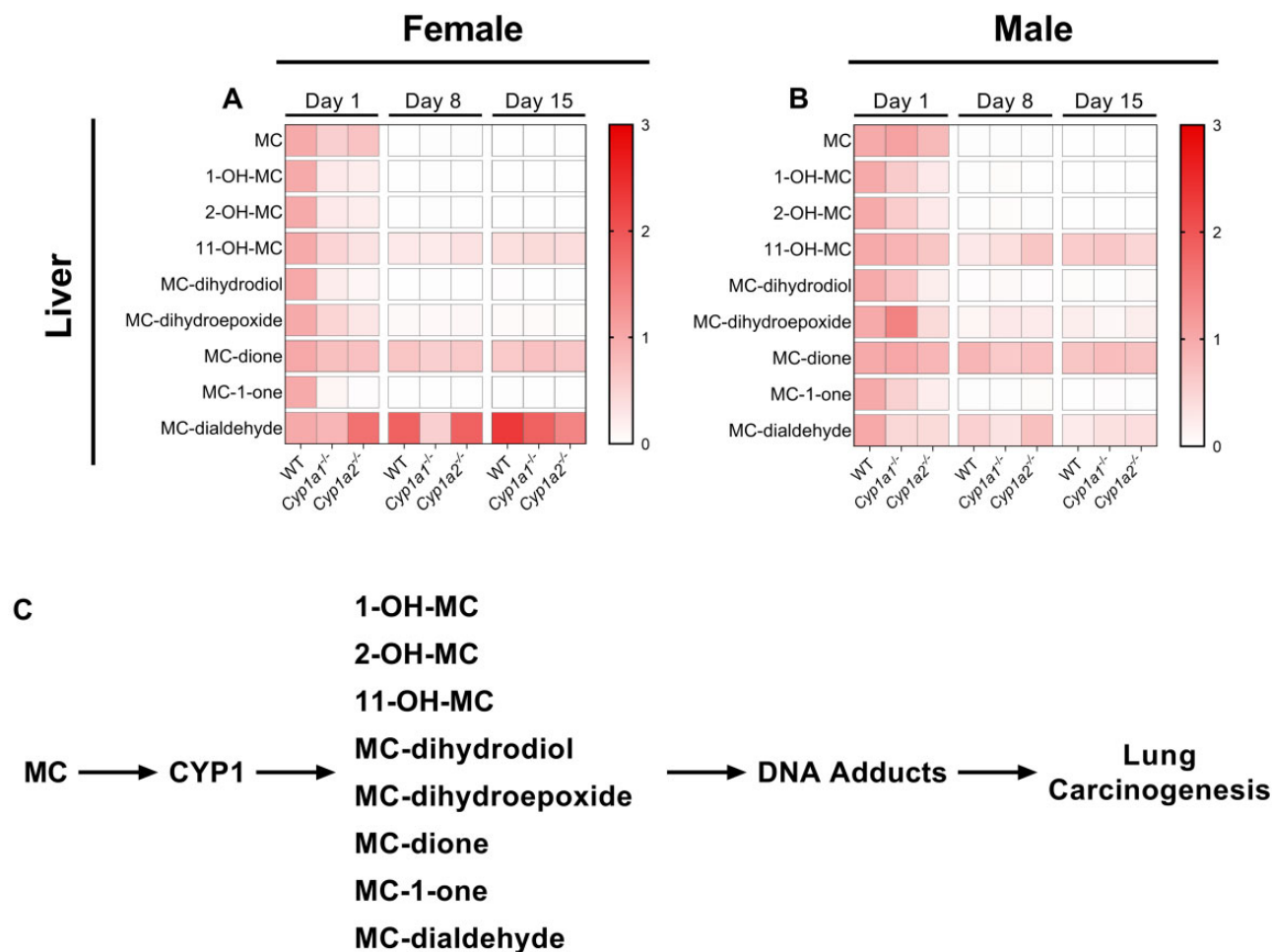

Figure 5. Differential hepatic metabolism of 3-methylcholanthrene (MC) in wild-type (WT), $Cyp1a1^{-/-}$, and $Cyp1a2^{-/-}$ mice. Female (A) and male (B) hepatic metabolomics. Schematic of CYP1-derived metabolites and their relation to pulmonary carcinogenesis (C). All compounds are normalized to their respective WT day 1 timepoints. Significant differences between groups are shown in Supplementary Table 1.
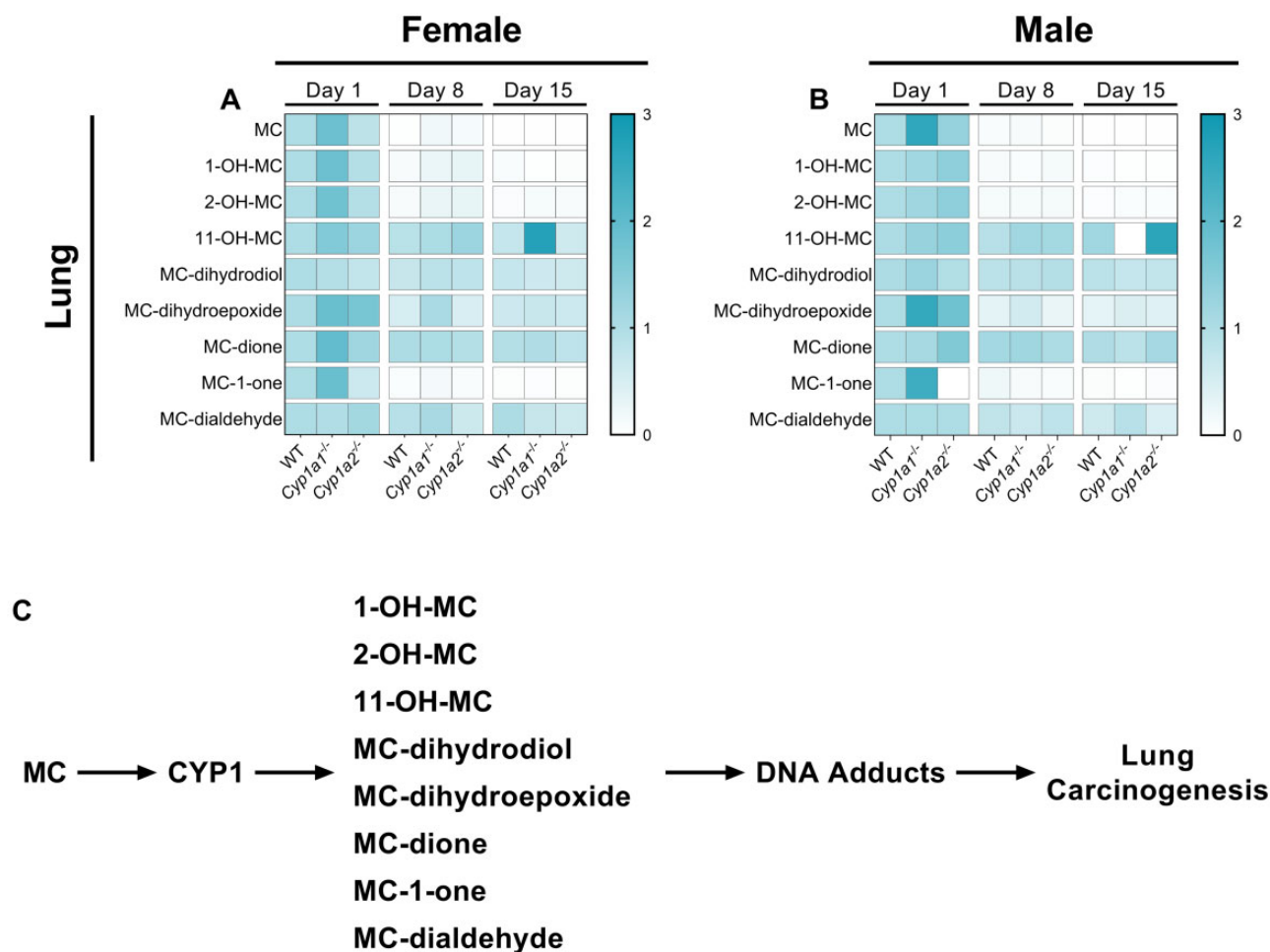
Figure 6. Differential pulmonary metabolism of 3-methylcholanthrene (MC) in wild-type (WT), $Cyp1a1^{-/-}$, and $Cyp1a2^{-/-}$ mice. Female (A) and male (B) pulmonary metabolomics. Schematic of CYP1-derived metabolites and their relation to pulmonary carcinogenesis (C). All compounds are normalized to their respective WT day 1 timepoints. Significant differences between groups are shown in Supplementary Table 1.

6). A complete summary of the statistical analysis performed for all comparisons can be found in Supplementary Table 1. Regarding the parent compound, we found that female $Cyp1a1^{-/-}$ mice had lower hepatic levels of MC ($p = .02$) than WT mice (Figure 5A) whereas male $Cyp1a1^{-/-}$ mice displayed increased pulmonary levels of MC (Figure 6B; $p = .010$). Analysis of the 1- and 2-hydroxy metabolites revealed that female $Cyp1a1^{-/-}$ mice had lower hepatic levels of both 1- and 2-hydroxy-MC ($p = .022$). Similarly, female $Cyp1a2^{-/-}$ mice also displayed reduced hepatic levels of 1- and 2-hydroxy-MC ($p = .015$). However, only male $Cyp1a2^{-/-}$ mice displayed a decrease in hepatic 1- ($p = .019$) and 2-hydroxy-MC ($p = .020$) (Figs. 5A and 5B). Both female $Cyp1a1^{-/-}$ and $Cyp1a2^{-/-}$ mice had significantly lower hepatic levels of MC-11,12-dihydrodiol ($p = .033$; $p = .014$, respectively) and MC-11,12-dione ($p = .023$; $p = .0019$, respectively) at 1-day post exposure (Figure 5A). In addition, female $Cyp1a2^{-/-}$ mice had lower levels of hepatic 11-hydroxy-MC ($p = .029$), MC-11,12-dihydroepoxide ($p = .019$), and MC-1-one ($p = .049$) compared with WT mouse livers (Figure 5A). Male $Cyp1a1^{-/-}$ and $Cyp1a2^{-/-}$ mice had increased hepatic MC-11,12-dialdehyde ($p = .01$; $p = .0069$, respectively); however, the 2 groups of mice differed in their hepatic MC-11,12-dihydroepoxide levels with $Cyp1a1^{-/-}$ mice harboring higher levels ($p = .041$) and $Cyp1a2^{-/-}$ mice harboring lower levels ($p = .01$) compared with WT mice (Figure 5B).

We also observed sex-specific differences in the pulmonary metabolomics of PAHs in the mice. Compared with WT mice, female $Cyp1a1^{-/-}$ mice showed increased MC-1-one ($p = .046$) and 11-hydroxy-MC ($p = .0069$) levels at 1- and 15-days post exposure, respectively (Figure 6A). Interestingly, male $Cyp1a2^{-/-}$ mice had increased MC-1-one ($p = .004$) levels 1-day post exposure (Figure 6B). Male $Cyp1a1^{-/-}$ mice showed a significant increase in MC-11,12-dihydroepoxide ($p = .0043$) and MC-11,12-dihydrodiol ($p = .0072$) compared with WT mice (Figure 6B).

PAH-induced Tumor Multiplicity and Incidence

WT, $Cyp1a1^{-/-}$ and $Cyp1a2^{-/-}$ mice were treated with MC (40 µmol/kg) via ip injection and sacrificed 8-month post-MC exposure for tumor multiplicity and incidence analysis. We found that $Cyp1a2^{-/-}$ mice had a significantly higher tumor burden than WT mice (Figure 7A) with male mice showing a 99% increase ($p < .0001$) and female mice showing a 219% increase ($p < .0001$) in tumor burden. Despite the increase in DNA adducts seen in female $Cyp1a1^{-/-}$ mice earlier (Figure 3B), $Cyp1a1^{-/-}$ mice harbored significantly fewer lung tumors than WT mice with female mice showing a 70% decrease ($p = .0003$) and male mice showing a 68% decrease ($p = .017$) in tumors (Figure 7A). MC resulted in a high incidence of tumors within all genotypes, whereas vehicle-treated animals had a low tumor
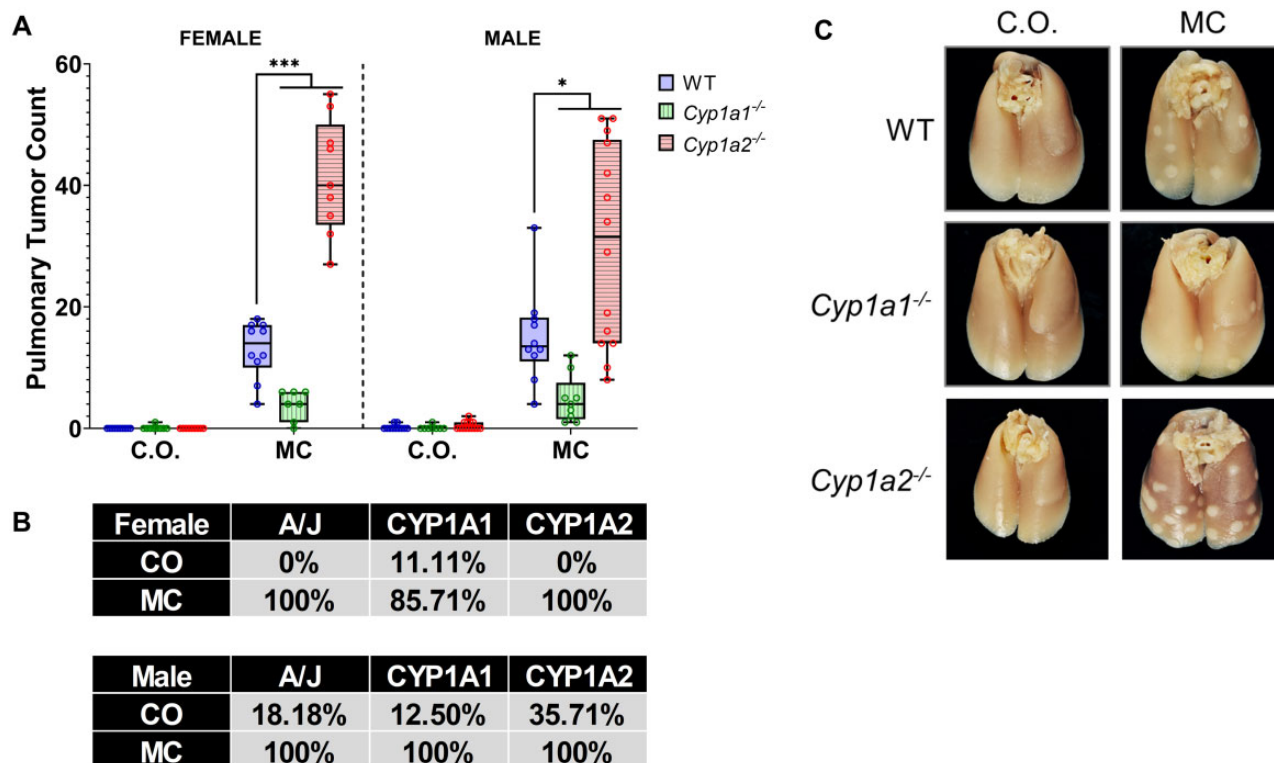
Figure 7. 3-Methylcholanthrene (MC)-induced pulmonary tumor formation study. Tumor multiplicity (A) and tumor incidence (B) analysis ($n = 7–14$). Representative pictures of lungs from each treatment group (C). Dunnett's multiple comparisons test was used to analyze the tumor multiplicity data. Significant differences between wild-type (WT) and knockout mice at each timepoint are indicated by *$p < .05$, **$p < .01$, and ***$p < .001$. The tumor incidence values represent the percentage of mice that developed lung tumors in each group. Abbreviation: CO, corn oil.

incidence (Figure 7B). Representative pictures of the lungs used in our analysis are provided (Figure 7C).

Effect of CYP1A2 on LUAD Patient Survival

We utilized the UALCAN online resource to analyze TCGA RNA expression data from lung cancer patients. Specifically, we wanted to determine whether either CYP1A1 or 1A2 expression had an effect on patient survival. We found that high expression of CYP1A2 in LUADs gave patients a survival advantage (Figure 8A; $p = .0059$), compared with patients with low/medium CYP1A2 expression. Interestingly, when we analyzed male and female patients separately, we found that only male patients retained the survival benefit (Figure 8C; $p = .0083$) while female patients expressing high levels of CYP1A2 did not (Figure 8B; $p = .22$).

DISCUSSION

In this study, we investigated the specific roles of CYP1A1 and 1A2 in PAH-mediated pulmonary carcinogenesis using $Cyp1a1^{-/-}$ and $Cyp1a2^{-/-}$ mouse models. We hypothesized that mice lacking the $Cyp1a1$ gene would be less susceptible to PAH-induced lung cancer while mice lacking the $Cyp1a2$ gene would be more susceptible.

Our findings (Figure 1) suggest that absence of one of the CYP1A genes leads to higher degree of induction of the other CYP1A gene, probably as a compensatory response to deal with the increased PAH burden. In addition, this compensatory response could be the cause of the increased EROD activity we observed in the livers of the $Cyp1a1^{-/-}$ mice (Figs. 1B and 1I). EROD is relatively specific for CYP1A1 activity in WT animals;

however, because the CYP1A enzymes have overlapping substrate specificities and CYP1A2 expression is elevated in $Cyp1a1^{-/-}$ mice, we believe that CYP1A2-dependent metabolism was responsible for the EROD activity. Our finding that both male and female $Cyp1a2^{-/-}$ mice displayed an increase in pulmonary CYP1A1 RNA and protein expression, and EROD activity when compared with WT mice for up to 8 days (Figure 2) supports the idea that MC elicits prolonged expression of CYP1A1 (Moorthy, 2000). These studies were consistent with our earlier work, which showed that CYP1A2 suppresses endogenous as well as inducible CYP1A1 expression. This suggests a regulatory role for CYP1A2 on CYP1A1 gene expression (Jiang et al., 2010; Kondraganti et al., 2002).

The formation of DNA adducts in male and female mice treated with MC for up to 15 days (Figure 3) was in agreement with earlier studies showing the formation of DNA-reactive metabolites in mice after MC exposure (Kondraganti et al., 2003; Lu et al., 1990; Wood et al., 1978). The fact that $Cyp1a1^{-/-}$ mice showed lower levels of adducts than WT mice supported the hypothesis that CYP1A1 played an important role in the metabolic activation of MC to DNA-binding metabolites (Kondraganti et al., 2003; Lu et al., 1990; Moorthy et al., 2015; Wood et al., 1978). Although MC forms multiple DNA adducts (Figure 3), spots 7 and 8 in our study probably represented the ultimate carcinogenic metabolites, 7,8-epoxy-7,8,9,10-tetrahydro-(1 or 2), and 7,8-epoxy-7,8,9,10-tetrahydro-(1 or 2), 9,10-trihydroxy-3-hydroxy-MC, respectively, based on their similar chromatographic profiles according to ^{32}P-postlabeling (Figure 3) (Lu et al., 1990; Wood et al., 1978). The significantly decreased levels of spots 7 and 8 in $Cyp1a1$-null mice (Supplementary Figure 1) lends further credence to the hypothesis that CYP1A1 plays a pivotal role

Effect of CYP1A2 expression on LUAD patient survival

Effect of CYP1A2 expression and gender on LUAD patient survival
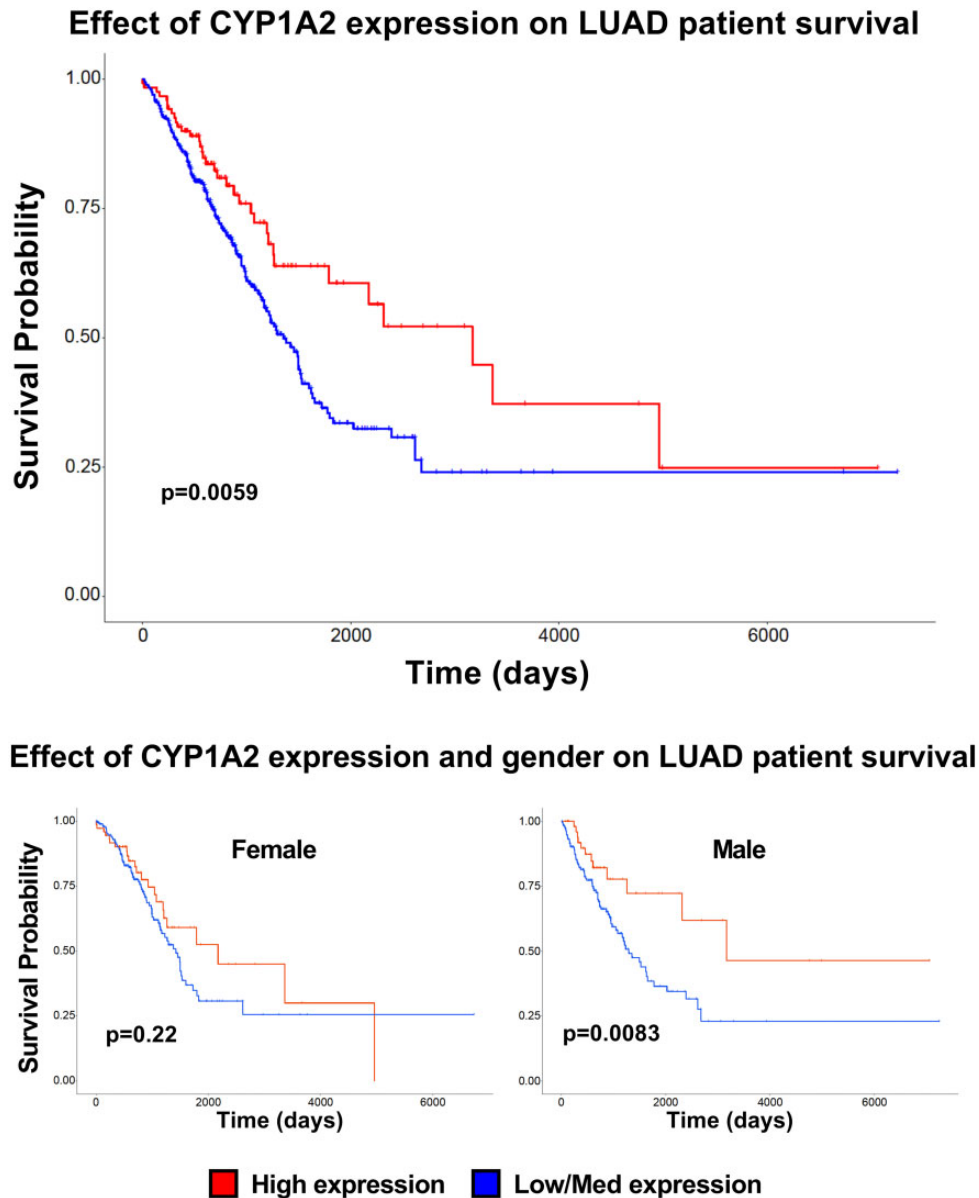

Figure 8. Effect of CYP1A2 expression level on lung adenocarcinoma (LUAD) patient survival. UALCAN was used to analyze the effect of CYP1A2 expression on LUAD patient survival. Kaplan-Meier plot of patients with high (red) versus medium/low (blue) CYP1A2 RNA expression (A). The effect of gender and CYP1A2 expression is plotted for female (B) and male (C) patients.

in the formation of the ultimate carcinogenic metabolites. The augmentation of total MC-DNA adduct levels in $Cyp1a2^{-/-}$ mice (Figure 3), in regard to WT mice, supported the hypothesis that CYP1A2 protects against MC-mediated carcinogenesis. The fact that the levels of DNA adduct spots 7 and 8 were much higher in $Cyp1a2^{-/-}$ mice than WT mice (Supplementary Figure 1) provides further evidence of the anticarcinogenic role of CYP1A2. Although we did see a significant increase in pulmonary DNA adducts in female mice, our tumor study revealed these specific adducts do not cause significant tumor formation in our animals. Our metabolomics analysis revealed that some metabolites, such as 11-hydroxy-MC, were elevated in female $Cyp1a1^{-/-}$ mice. We hypothesize that sex-specific differences in CYP1A expression cause the differential production of reactive metabolites that are in turn responsible for differences in DNA adduct formation and tumorigenesis. This phenomenon may also be

due to the third CYP1 enzyme, $Cyp1b1$. Studies have shown that estradiol (E_2) can induce CYP1B1 expression through estrogen receptor alpha, which can bind estrogen response elements found in the $Cyp1b1$ promoter (Tsuchiya et al., 2004).

Next, we investigated the phase II enzyme, NQO1 (Figure 4), which is known to be induced by MC treatment (Jin et al., 2014). Although $Cyp1a1^{-/-}$ mice showed sex-specific differences, both male and female mice tended to have a robust pulmonary NQO1 response that may have contributed to the decrease in lung carcinogenesis and tumor formation seen in this genotype. Hepatic NQO1 RNA was also elevated in $Cyp1a1^{-/-}$ mice (Supplementary Figure 2). Furthermore, the pulmonary NQO1 response in $Cyp1a2^{-/-}$ mice was limited to an increase in RNA expression compared with baseline levels at 1-day post exposure and the hepatic response resulted in the level of NQO1 protein being higher than that in WT controls for only a single day.
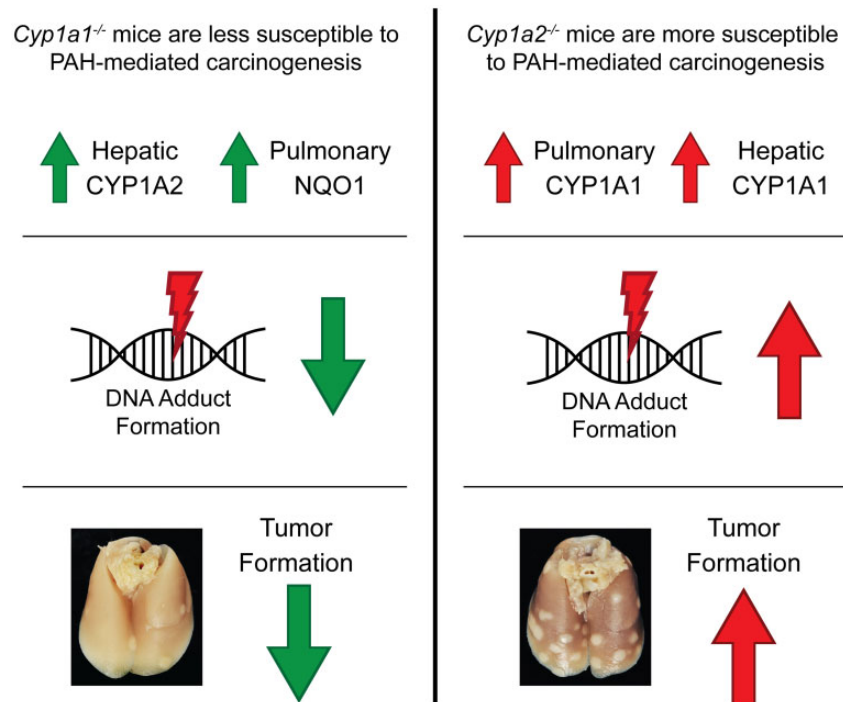
Figure 9. Possible mechanisms underlying the differential susceptibilities of *Cyp1a1*$^{-/-}$ and *Cyp1a2*$^{-/-}$ mice to polycyclic aromatic hydrocarbon (PAH)-mediated pulmonary tumorigenesis. The above diagram outlines the major findings and potential mechanisms that could contribute to the different levels of pulmonary carcinogenesis observed in *Cyp1a1*$^{-/-}$ and *Cyp1a2*$^{-/-}$ mice. (Left) *Cyp1a1*$^{-/-}$ mice displayed increased hepatic CYP1A2 and pulmonary NQO1 expression, compared with wild-type mice. This could contribute to the decrease in pulmonary DNA adduct formation and tumorigenesis observed in these mice. (Right) *Cyp1a2*$^{-/-}$ mice displayed a compensatory hepatic and pulmonary CYP1A1 response. This may contribute to the significantly higher levels of hepatic DNA adducts and pulmonary tumor multiplicity observed in these mice.

These data suggest that the reduction in tumors seen in *Cyp1a1*$^{-/-}$ mice may be in part due to the observed NQO1 response, which was not seen in *Cyp1a2*$^{-/-}$ mice.

In regard to MC metabolomics (Figs. 5 and 6), we found that *Cyp1a1*$^{-/-}$ female mice had significantly lower levels of hepatic MC, 1-OH-MC, and 2-OH-MC compared with WT mice. Although male mice displayed a similar downward trend for the levels of 1-OH-MC, and 2-OH-MC, they were not significantly lower than the WT levels. Pulmonary metabolic analysis revealed that male *Cyp1a1*$^{-/-}$ mice had significantly higher levels of the parent compound (MC) than WT mice, whereas female mice showed a similar trend ($p = .1170$). This suggests that in *Cyp1a1*$^{-/-}$ mice, hepatic CYP1A2 may metabolize more of the parent compound to nontoxic metabolites, leading to decreased carcinogenesis. Next, we found that *Cyp1a1*$^{-/-}$ and *Cyp1a2*$^{-/-}$ mice had an increased level of pulmonary MC-1-one compared with WT controls (Figs. 6A and 6B). Metabolism of MC to metabolites such as MC-1-one, is known to increase reactive oxygen species levels as well as NQO1 expression in mice (Jin et al., 2014). Because NQO1 has been shown to be important for mitigating PAH-induced carcinogenesis (Shen et al., 2010) and the *Cyp1a1*$^{-/-}$ mice showed a robust NQO1 response to MC treatment, it is possible that MC-1-one is one of the relevant carcinogenic metabolites of MC.

Our tumor studies showing the formation of lung tumors in MC-treated A/J mice were in agreement with earlier work on lung tumorigenesis caused by MC (O'Donnell et al., 2006). We found a decrease in tumor multiplicity in *Cyp1a1*$^{-/-}$ mice, and an increase in *Cyp1a2*$^{-/-}$ mice (Figure 7). These findings show that the absence of CYP1A1 leads to a significant decrease in PAH-induced lung tumor formation, whereas the absence of CYP1A2 leads to a significant increase in PAH-induced lung tumor formation. This supports our hypothesis that CYP1A1 and 1A2 play opposing roles in MC-mediated carcinogenesis, with CYP1A1 playing a role as an inducer of carcinogenesis and CYP1A2 playing a role as an anticarcinogen. This is a novel observation that is paradigm shifting and additional studies will be required to investigate the mechanisms of the opposing roles of these 2 members of the CYP1A subfamily in PAH-mediated lung carcinogenesis.

Finally, we investigated whether these newly discovered roles of CYP1A1 and 1A2 were observed in humans. To do so, we examined the effect of CYP1A1 or 1A2 expression on LUAD patient survival (Figure 8). We found that LUAD patients with high CYP1A2 expression in their primary tumors survived longer than patients with low/medium expression in their primary tumors. This corresponds well with our mouse study, because our *Cyp1a1*$^{-/-}$ mice, which retain CYP1A2 function, developed significantly fewer pulmonary tumors. Interestingly, when we investigated the effect of sex on this correlation, we found that high CYP1A2 expression conferred a survival advantage to male patients, but in females, it did not. These findings correspond to those of previous studies (Kiyohara and Ohno, 2010; Mollerup et al., 1999; Uppstad et al., 2011) and highlight the translational value of this study.

In conclusion, our data support the hypothesis that mice lacking the *Cyp1a1* gene are less susceptible to PAH-induced lung cancer while mice lacking the *Cyp1a2* gene are more susceptible (Figure 9). We were able to show that *Cyp1a2*$^{-/-}$ mice had increased susceptibility to hepatic and pulmonary DNA adduct formation, whereas male *Cyp1a1*$^{-/-}$ mice were resistant to pulmonary DNA adduct formation. Together, these data support

our hypothesis in terms of cancer initiation (DNA adduct formation) as well as pulmonary tumorigenesis (tumor multiplicity). In addition, CYP1A1/1A2 RNA and protein analysis showed that when 1 gene was knocked out, the other responded in a compensatory manner. This suggests that the differences seen in tumor formation could be due not only to the absence of each gene, but also to the increased activity of the other. Efforts to determine the pulmonary and hepatic metabolomics also revealed genotype- and sex-specific differences and that, MC-1-one, a substrate of NQO1, is a potential critical metabolite. NQO1 RNA and protein analysis revealed that $Cyp1a1^{-/-}$ mice had a more robust NQO1 response than their $Cyp1a2^{-/-}$ counterparts. This suggests that the alteration of the metabolomics as well as the way in which the knockout mice handled the different levels of MC metabolites could play a role in the resistance or susceptibility to PAH-induced lung cancer seen in these animals.

Future studies in our laboratory will support efforts to develop CYP1A1 inhibitors to combat PAH-induced carcinogenesis in high-risk populations. Such efforts include the development of synthetic CYP1A inhibitors, such as the heterocyclic chalcone (E)-3-(3,4,5-trimethoxyphenyl)-1-(pyridin-4-yl)prop-2-en-1-one (Horley *et al.*, 2017). Although this compound inhibits both CYP1A enzymes, it has a 10-fold greater selectivity toward CYP1A1 than CYP1A2 and CYP1B1, highlighting its therapeutic potential as a selective CYP1A1 inhibitor.

SUPPLEMENTARY DATA

Supplementary data are available at *Toxicological Sciences* online.

ACKNOWLEDGMENT

FUNDING

DECLARATION OF CONFLICTING INTERESTS

The authors declared no potential conflicts of interest with respect to the research, authorship, and/or publication of this article.

REFERENCES

American Cancer Society. (2019). *Cancer Facts & Figures 2019*. American Cancer Society, Atlanta.

Ben-Zaken Cohen, S., Pare, P. D., Man, S. F., and Sin, D. D. (2007). The growing burden of chronic obstructive pulmonary disease and lung cancer in women: Examining sex differences in cigarette smoke metabolism. *Am. J. Respir. Crit. Care Med.* **176**, 113–120.

Ceppi, M., Munnia, A., Cellai, F., Bruzzone, M., and Peluso, M. E. M. (2017). Linking the generation of DNA adducts to lung cancer. *Toxicology* **390**, 160–166.

Chandrashekar, D. S., Bashel, B., Balasubramanya, S. A. H., Creighton, C. J., Ponce-Rodriguez, I., Chakravarthi, B. V. S. K., and Varambally, S. (2017). UALCAN: A portal for facilitating tumor subgroup gene expression and survival analyses. *Neoplasia* **19**, 649–658.

Cinti, D. L., Moldeus, P., and Schenkman, J. B. (1972). Kinetic parameters of drug-metabolizing enzymes in Ca^{2+}-sedimented microsomes from rat liver. *Biochem. Pharmacol.* **21**, 3249–3256.

Fazili, I. S., Jiang, W., Wang, L., Felix, E. A., Khatlani, T., Coumoul, X., Barouki, R., and Moorthy, B. (2010). Persistent induction of cytochrome P4501A1 in human hepatoma cells by 3-methylcholanthrene: Evidence for sustained transcriptional activation of the CYP1A1 promoter. *J. Pharmacol. Exp. Ther.* **333**, 99–109.

Goldstone, H. M., and Stegeman, J. J. (2006). A revised evolutionary history of the CYP1A subfamily: Gene duplication, gene conversion, and positive selection. *J. Mol. Evol.* **62**, 708–717.

Grimmer, G., Brune, H., Dettbarn, G., Naujack, K. W., Mohr, U., and Wenzel-Hartung, R. (1988). Contribution of polycyclic aromatic compounds to the carcinogenicity of sidestream smoke of cigarettes evaluated by implantation into the lungs of rats. *Cancer Lett.* **43**, 173–177.

Harvey, R. G. (1982). Polycyclic hydrocarbons and cancer. *Am. Sci.* **70**, 386–393.

Hecht, S. S. (2003). Tobacco carcinogens, their biomarkers and tobacco-induced cancer. *Nat. Rev. Cancer* **3**, 733–744.

Hecht, S. S. (2012). Lung carcinogenesis by tobacco smoke. *Int. J. Cancer* **131**, 2724–2732.

Henry, C. J., Billups, L. H., Avery, M. D., Rude, T. H., Dansie, D. R., Lopez, A., Sass, B., Whitmire, C. E., and Kouri, R. E. (1981). Lung cancer model system using 3-methylcholanthrene in inbred strains of mice. *Cancer Res.* **41**, 5027–5032.

Horley, N. J., Beresford, K. J. M., Kaduskar, S., Joshi, P., McCann, G. J. P., Ruparelia, K. C., Williams, I. S., Gatchie, L., Sonawane, V. R., Bharate, S. B., *et al.* (2017). (E)-3-(3,4,5-Trimethoxyphenyl)-1-(pyridin-4-yl)prop-2-en-1-one, a heterocyclic chalcone is a potent and selective CYP1A1 inhibitor and cancer chemopreventive agent. *Bioorg. Med. Chem. Lett.* **27**, 5409–5414.

Jiang, W., Wang, L., Kondraganti, S. R., Fazili, I. S., Couroucli, X. I., Felix, E. A., and Moorthy, B. (2010). Disruption of the gene for CYP1A2, which is expressed primarily in liver, leads to differential regulation of hepatic and pulmonary mouse CYP1A1 expression and augmented human CYP1A1 transcriptional activation in response to 3-methylcholanthrene *in vivo*. *J. Pharmacol. Exp. Ther.* **335**, 369–379.

Jin, Y., Miao, W., Lin, X., Pan, X., Ye, Y., Xu, M., and Fu, Z. (2014). Acute exposure to 3-methylcholanthrene induces hepatic oxidative stress via activation of the Nrf2/ARE signaling pathway in mice. *Environ. Toxicol.* **29**, 1399–1408.

Jorge-Nebert, L. F., Jiang, Z., Chakraborty, R., Watson, J., Jin, L., McGarvey, S. T., Deka, R., and Nebert, D. W. (2010). Analysis of human CYP1A1 and CYP1A2 genes and their shared bidirectional promoter in eight world populations. *Hum. Mutat.* **31**, 27–40.

Juvonen, R. O., Jokinen, E. M., Javaid, A., Lehtonen, M., Raunio, H., and Pentikäinen, O. T. (2020). Inhibition of human CYP1 enzymes by a classical inhibitor α-naphthoflavone and a novel

inhibitor N-(3,5-dichlorophenyl)cyclopropanecarboxamide—An *in vitro* and *in silico* study. *Chem. Biol. Drug Des.* **95**, 520–533.

Kiyohara, C., and Ohno, Y. (2010). Sex differences in lung cancer susceptibility: A review. *Gend. Med.* **7**, 381–401.

Kondraganti, S. R., Fernandez-Salguero, P., Gonzalez, F. J., Ramos, K. S., Jiang, W., and Moorthy, B. (2003). Polycyclic aromatic hydrocarbon-inducible DNA adducts: Evidence by ^{32}P-postlabeling and use of knockout mice for Ah receptor-independent mechanisms of metabolic activation *in vivo*. *Int. J. Cancer* **103**, 5–11.

Kondraganti, S. R., Jiang, W., and Moorthy, B. (2002). Differential regulation of expression of hepatic and pulmonary cytochrome P4501A enzymes by 3-methylcholanthrene in mice lacking the CYP1A2 gene. *J. Pharmacol. Exp. Ther.* **303**, 945–951.

Lingappan, K., Jiang, W., Wang, L., Couroucli, X. I., Barrios, R., and Moorthy, B. (2013). Sex-specific differences in hyperoxic lung injury in mice: Implications for acute and chronic lung disease in humans. *Toxicol. Appl. Pharmacol.* **272**, 281–290.

Lu, L. J., Harvey, R. G., Lee, H., Baxter, J. R., and Anderson, L. M. (1990). Age-, tissue-, and Ah genotype-dependent differences in the binding of 3-methylcholanthrene and its metabolite(s) to mouse DNA. *Cancer Res.* **50**, 4239–4247.

Matsubara, T., Prough, R. A., Burke, M. D., and Estabrook, R. W. (1974). The preparation of microsomal fractions of rodent respiratory tract and their characterization. *Cancer Res.* **34**, 2196–2203.

Mollerup, S., Ryberg, D., Hewer, A., Phillips, D. H., and Haugen, A. (1999). Sex differences in lung CYP1A1 expression and DNA adduct levels among lung cancer patients. *Cancer Res.* **59**, 3317–3320.

Moorthy, B. (2000). Persistent expression of 3-methylcholanthrene-inducible cytochromes P4501A in rat hepatic and extrahepatic tissues. *J. Pharmacol. Exp. Ther.* **294**, 313–322.

Moorthy, B., Chen, S., Li, D., and Randerath, K. (1993). 3-Methylcholanthrene-inducible liver cytochrome(s) P450 in female Sprague-Dawley rats: Possible link between P450 turnover and formation of DNA adducts and I-compounds. *Carcinogenesis* **14**, 879–886.

Moorthy, B., Chu, C., and Carlin, D. J. (2015). Polycyclic aromatic hydrocarbons: From metabolism to lung cancer. *Toxicol. Sci.* **145**, 5–15.

Moorthy, B., Nguyen, U. T., Gupta, S., Stewart, K. D., Welty, S. E., and Smith, C. V. (1997). Induction and decline of hepatic cytochromes P4501A1 and 1A2 in rats exposed to hyperoxia are not paralleled by changes in glutathione S-transferase-alpha. *Toxicol. Lett.* **90**, 67–75.

National Research Council. (1983). *Polycyclic Aromatic Hydrocarbons: Evaluation of Sources and Effects*. National Academies Press, Washington, DC. Available at: https://doi.org/10.17226/738

Nebert, D. W., Shi, Z., Galvez-Peralta, M., Uno, S., and Dragin, N. (2013). Oral benzo[a]pyrene: Understanding pharmacokinetics, detoxication, and consequences-Cyp1 knockout mouse lines as a paradigm. *Mol. Pharmacol.* **84**, 304–313.

Nukaya, M., and Bradfield, C. A. (2009). Conserved genomic structure of the CYP1A1 and CYP1A2 loci and their dioxin responsive elements cluster. *Biochem. Pharmacol.* **77**, 654–659.

O'Donnell, E. P., Zerbe, L. K., Dwyer-Nield, L. D., Kisley, L. R., and Malkinson, A. M. (2006). Quantitative analysis of early chemically-induced pulmonary lesions in mice of varying susceptibilities to lung tumorigenesis. *Cancer Lett.* **241**, 197–202.

Phillips, T. D., Richardson, M., Cheng, Y. S., He, L., McDonald, T. J., Cizmas, L. H., Safe, S. H., Donnelly, K. C., Wang, F., Moorthy, B., *et al.* (2015). Mechanistic relationships between

hepatic genotoxicity and carcinogenicity in male B6C3F1 mice treated with polycyclic aromatic hydrocarbon mixtures. *Arch. Toxicol.* **89**, 967–977.

Poirier, M. C., and Beland, F. A. (1992). DNA adduct measurements and tumor incidence during chronic carcinogen exposure in animal models: Implications for DNA adduct-based human cancer risk assessment. *Chem. Res. Toxicol.* **5**, 749–755.

Pokhrel, B., Gong, P., Wang, X., Wang, C., and Gao, S. (2018). Polycyclic aromatic hydrocarbons in the urban atmosphere of Nepal: Distribution, sources, seasonal trends, and cancer risk. *Sci. Total Environ.* **618**, 1583–1590.

Reddy, M. V., and Randerath, K. (1986). Nuclease P1-mediated enhancement of sensitivity of ^{32}P-postlabeling test for structurally diverse DNA adducts. *Carcinogenesis* **7**, 1543–1551.

Shen, J., Barrios, R. J., and Jaiswal, A. K. (2010). Inactivation of the quinone oxidoreductases NQO1 and NQO2 strongly elevates the incidence and multiplicity of chemically induced skin tumors. *Cancer Res.* **70**, 1006–1014.

Shi, J., Zheng, G. J., Wong, M. H., Liang, H., Li, Y., Wu, Y., Li, P., and Liu, W. (2016). Health risks of polycyclic aromatic hydrocarbons via fish consumption in Haimen bay (China), downstream of an e-waste recycling site (Guiyu). *Environ. Res.* **147**, 233–240.

Simko, P. (2002). Determination of polycyclic aromatic hydrocarbons in smoked meat products and smoke flavouring food additives. *J. Chromatogr. B Anal. Technol. Biomed. Life Sci.* **770**, 3–18.

Singh, S. V., Benson, P. J., Hu, X., Pal, A., Xia, H., Srivastava, S. K., Awasthi, S., Zaren, H. A., Orchard, J. L., and Awasthi, Y. C. (1998). Gender-related differences in susceptibility of A/J mouse to benzo[a]pyrene-induced pulmonary and forestomach tumorigenesis. *Cancer Lett.* **128**, 197–204.

Stiborová, M., Moserová, M., Černá, V., Indra, R., Dračínský, M., Šulc, M., Henderson, C. J., Wolf, C. R., Schmeiser, H. H., Phillips, D. H., *et al.* (2014). Cytochrome b5 and epoxide hydrolase contribute to benzo[a]pyrene-DNA adduct formation catalyzed by cytochrome P450 1A1 under low NADPH: P 450 oxidoreductase conditions. *Toxicology* **318**, 1–12.

Tang, D., Phillips, D. H., Stampfer, M., Mooney, L. A., Hsu, Y., Cho, S., Tsai, W. Y., Ma, J., Cole, K. J., She, M. N., *et al.* (2001). Association between carcinogen-DNA adducts in white blood cells and lung cancer risk in the physicians health study. *Cancer Res.* **61**, 6708–6712.

Tsuchiya, Y., Nakajima, M., Kyo, S., Kanaya, T., Inoue, M., and Yokoi, T. (2004). Human CYP1B1 is regulated by estradiol via estrogen receptor. *Cancer Res.* **64**, 3119–3125.

Uno, S., Dalton, T. P., Dragin, N., Curran, C. P., Derkenne, S., Miller, M. L., Shertzer, H. G., Gonzalez, F. J., and Nebert, D. W. (2006). Oral benzo[a]pyrene in Cyp1 knockout mouse lines: CYP1A1 important in detoxication, CYP1B1 metabolism required for immune damage independent of total-body burden and clearance rate. *Mol. Pharmacol.* **69**, 1103–1114.

Uppstad, H., Osnes, G. H., Cole, K. J., Phillips, D. H., Haugen, A., and Mollerup, S. (2011). Sex differences in susceptibility to PAHs is an intrinsic property of human lung adenocarcinoma cells. *Lung Cancer* **71**, 264–270.

Vaz, M., Hwang, S. Y., Kagiampakis, I., Phallen, J., Patil, A., O'Hagan, H. M., Murphy, L., Zahnow, C. A., Gabrielson, E., Velculescu, V. E., *et al.* (2017). Chronic cigarette smoke-induced epigenomic changes precede sensitization of bronchial epithelial cells to single-step transformation by KRAS mutations. *Cancer Cell* **32**, 360–376.e6.

Wood, A. W., Chang, R. L., Levin, W., Thomas, P. E., Ryan, D., Stoming, T. A., Thakker, D. R., Jerina, D. M., and Conney, A. H.

(1978). Metabolic activation of 3-methylcholanthrene and its metabolites to products mutagenic to bacterial and mammalian cells. *Cancer Res.* **38**, 3398–3404.

World Health Organization (WHO) International Agency for Research on Cancer. (2004). *Tobacco Smoke and Involuntary Smoking. IARC Monographs on the Evaluation of Carcinogenic Risks to Humans* (S. Kaplan, Ed.), Vol. **83**, pp. 1179–1187. World Health Organization, Lyon, France.

Yeager, R. L., Reisman, S. A., Aleksunes, L. M., and Klaassen, C. D. (2009). Introducing the "TCDD-inducible AhR-Nrf2 gene battery". *Toxicol. Sci.* **111**, 238–246.

Zhou, G. D., Zhu, H., Phillips, T. D., Wang, J., Wang, S. Z., Wang, F., Amendt, B. A., Couroucli, X. I., Donnelly, K. C., and Moorthy, B. (2011). Effects of dietary fish oil on the depletion of carcinogenic PAH-DNA adduct levels in the liver of B6C3F1 mouse. *PLoS One* **6**, e26589.